DOI 10.1007/s12541-009-0063-7

Vibration Reduction Control of a Voice Coil Motor (VCM) Nano Scanner

Jong-kyu Jung[1], Woo-seub Youm[1] and Kyi-hwan Park[1,#]

1 Department of Mechatronics, Gwangju Institute Science and Technology, 1 Oryong dong, Buk gu, Gwangju, Korea, 500-712
Corresponding Author / E-mail: khpark@gist.ac.kr, TEL: +82-62-970-2391, FAX: +82-62-970-2384

KEYWORDS: 3D shape morphing, Template mesh, Implicit function, Mesh smoothing, Modified Laplacian coordinate

This paper presents vibration reduction control of a voice coil motor (VCM) nano scanner. We had developed a VCM scanner. The scanner has flexure hinges structure. However, the VCM nano scanner has some problems of thermal drift and small damping compared to the PZT driven nano scanner. Especially, the small damping coefficient of the VCM scanner causes mechanical vibration when the control input signal is near to the resonance frequencies. Additionally, disturbance to the VCM scanner and electronic noise in the sensor also cause the mechanical vibration when they are near to the resonant frequencies. The mechanical vibration reduces the servo bandwidth as well as the accuracy, which deteriorates the AFM image of the samples. We design a pre-filter to reduce the signal applied to the VCM nano scanner and electronic noise in the sensor whose frequency is closed the resonant frequency of the VCM nano scanner. We measure the time and frequency response of the VCM scanner without using the pre-filter and with using the pre-filter. Finally, the topology images of a bare wafer are measured and compared using the AFM.

Manuscript received: August 6, 2008 / Accepted: May 7, 2009

NOMENCLATURE

k = spring constant of the flexure hinge
m = mass of the VCM nano scanner
G_s (s)= transfer function of the VCM nano scanner
G_f(s)= transfer function of the pre-filter
$G_{scanner}$(s) = transfer function of the compensated scanner

1. Introduction

Recently, the application areas of nano technology are expanding to the various areas such as nano metrology, nano lithography, high density data recording, etc.[1-4] High precision x, y and z axis nano scanner are essential for these applications. Especially, for the industrial applications, nano scanners are required to have additional performances of wide working area, simple structure, reliability, and low cost in addition to the accuracy and servo bandwidth. PZT driven nano scanners have been conventionally applied to these applications since it provides high accuracy and wide bandwidth.[5-7] However, it has the disadvantage of short working range, control difficulty due to PZT hysteresis, creep and high cost.[8-10] These disadvantages give obstacles to expand to the industrial applications.

A nano scanner driven by Voice Coil Motor (VCM) draws a wide attention nowadays since it can solve the problems of the PZT. VCM provides a sufficient force to control the nano scanner with a high speed as well as large working range and easy control.[11-13] A VCM nano scanner is usually composed of permanent magnets, electromagnets, and flexure hinge structure. Using the Lorentz force generated between the permanent magnets and electromagnets, the flexure hinge structure moves proportionally to the applied current. This feature makes it easy to control without using closed loop feedback system.[14,15]

However, the VCM nano scanner has some problems of thermal drift and small damping compared to the PZT driven nano scanner. Especially, the small damping coefficient of the VCM scanner causes mechanical vibration when the control input signal is near to the resonance frequencies. Additionally, disturbance to the VCM scanner and electronic noise in the sensor also cause the mechanical vibration when they are near to the resonance frequencies. The

vibration problem is caused by the electromagnetic force applied to the mass-spring VCM scanning system. The mechanical vibration reduces the servo bandwidth as well as the accuracy, which deteriorates the AFM image of the samples.

In this paper, we propose a pre-filter to compensate the undesirable frequency response characteristic of the VCM nano scanner. The pre-filter attenuates the input signal applied to the VCM nano scanner whose frequency is close to the resonance frequencies of the VCM nano scanner.

To verify the performance of the designed the pre-filter, we measure the time and frequency responses of the VCM nano scanner. Finally, the topology images of a bare wafer is measured and compared using the AFM produced by Em4sys. Co. Ltd..

2. Static and dynamic characteristics of the VCM nano scanner

The schematic diagram of the VCM nano scanner is shown in Figure 1(a). The plate and flexures hinge can be simply modeled as a mass, m and spring, k respectively. Figure 1(b) shows the real configuration of the VCM nano scanner. The electromagnets attached to the plate drives the flexure hinge in the x and y directions using the Lorentz force generated between the permanent magnets and electromagnets.

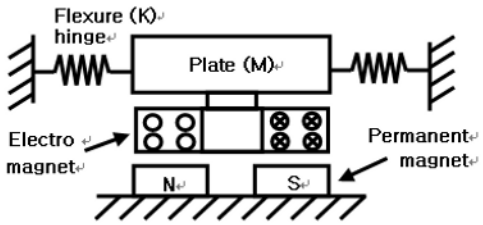

(a)

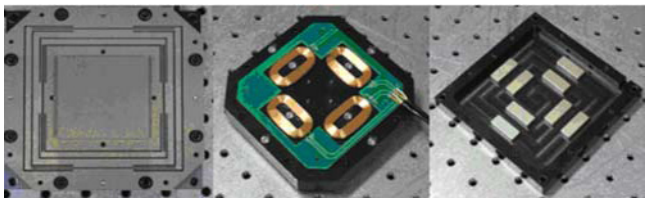

(b)

Fig. 1 The VCM nano scanner (a) schematic diagram, (b) the real configuration

The static characteristic of VCM is obtained by measuring the displacement for the applied current as shown in Figure 2(a) in which the displacement of the VCM has the linear characteristics for the applied current. It is one big advantage of using the VCM in contrast to the PZT actuator which has the hysteresis characteristic. The proportional relation with respect to the applied current makes it easy to control. Since the VCM nano scanner can be schematically modeled as a mass-spring system, it has the resonance characteristic as shown in Figure 2(b) [a black line and a red line]. The dynamic characteristic is measured by a laser vibrometer. Though the ideal VCM nano scanner can be modeled as a second order system, the measured frequency response shows that the VCM nano scanner has the secondary resonant frequency. It is attributed to the high order flexible or rigid body motion of the scanner.

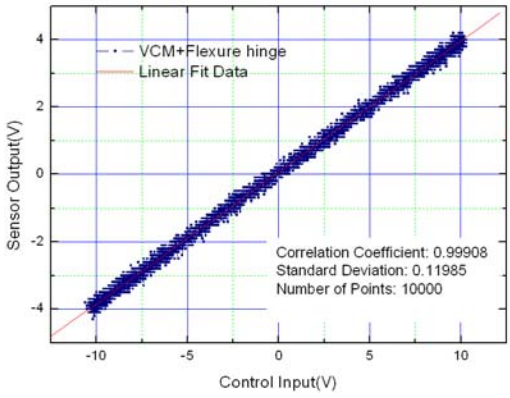

(a)

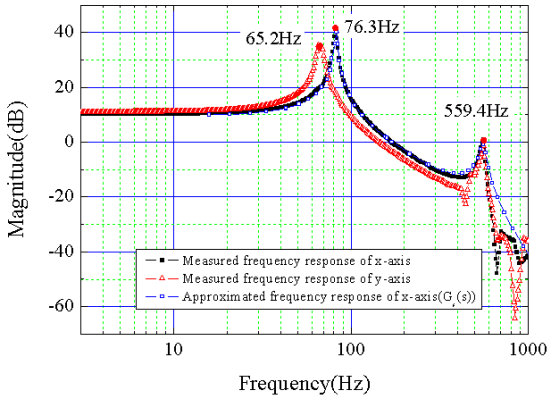

(b)

Fig. 2 (a) a static characteristic and (b) a dynamic characteristic of the VCM nano scanner

Then, the transfer function of the VCM nano scanner, $G_s(s)$ is represented in Eq. (1) [a blue line in the Figure 2(b)].

$$G_S(s) = \frac{5.67\times10^9}{S^4 + 51.4S^3 + 3.57\times10^5 S^2 + 1.239\times10^6 S + 1.885\times10^9} \quad (1)$$

The small damping coefficient of the VCM nano scanner causes mechanical vibration when the control input signal is near to the resonance frequencies. Additionally, electronic noise in the sensor also causes the mechanical vibration when they are near to the resonance frequencies of the nano scanner. The vibration problem is caused by the electromagnetic force applied to the mass-spring VCM scanning system. The mechanical vibration reduces the servo bandwidth as well as the accuracy, which deteriorates the AFM image of the samples.

3. Design of the pre-filter

We propose a pre-filter to solve the vibration problem. A pre-filter is designed to remove first and second modes of the nano scanner with the open loop frequency response of the nano scanner.

A blue line in the Figure 2(b) shows approximated frequency response in x-axis direction of the nano scanner. X and Y axis pre-filters as a kind of state variable filter can be considered each axis motion because each axis-motion of the nano scanner is decoupled. The pre-filter, G_f (s) has the form of

$$G_f(s) = \frac{5.69\times10^9 S^4 + 2.914\times10^{11} S^3 + 2.024\times10^{15} S^2 + 7.024\times10^{15} S + 1.069\times10^{19}}{5.69\times10^9 S^4 + 1.068\times10^{13} S^3 + 3.992\times10^{15} S^2 + 4.637\times10^{17} S + 1.069\times10^{19}} \quad (2)$$

Then, the feedforward gain of the compensated scanner, $G_{scanner}$ (s) is

$$G_{scanner}(s) = G_S(s)\times G_f(s) = \frac{5.67\times10^9}{S^4 + 1884S^3 + 7.04\times10^5 S^2 + 8.178\times10^7 S + 1.885\times10^9} \quad (3)$$

G_f and $G_{scanner}$ are shown in Figure 4.

Comparing the characteristic equation of the compensated VCM nano scanner, $G_{scanner}(S)$ in Eq. (3) with that of the original VCM nano scanner, $G_s(S)$ in Eq. (1), we can see the damping coefficients are increased from 0.0183 and 0.043 to 1.3625 and 1.5.

4. Experiments

Figure 3(a) shows the experimental result when the step input of 100um is applied to the VCM nano scanner in the x-direction without using the pre-filter is not used. The maximum magnitude of the vibration is almost 100nm. The frequency of the excited vibration is the same as the resonant frequency. Figure 3(b) shows the experimental result when the step input of 100um is applied to the VCM nano scanner in the x-direction with using the pre-filter. The vibration is decreased to lower than 10nm.

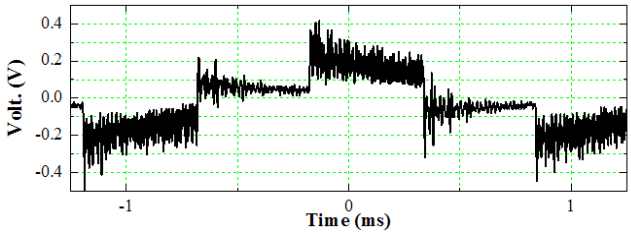

(a) when the pre-filter is not used

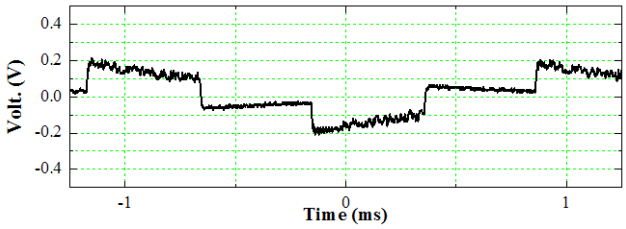

(b) when the pre-filter is used

Fig. 3 The measured step input response x-direction vibration

Fig. 4 shows the simulation results of the pre-filter and the compensated the VCM scanner for the x axis. It also shows the measured frequency response of the open loop system without and with pre-filter. The vibration magnitude of the scanner is about 38 dB at the first resonant frequency when the pre-filter is not used. However, the vibration magnitude of the scanner with using the pre-filter is reduced to below 3 dB when the pre-filter is used. From these results, we can verify that the resonance effects are disappeared.

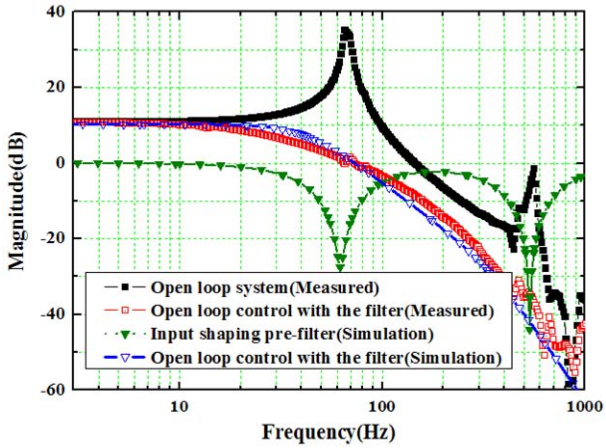

Fig. 4 The x-axis frequency response and simulation result of the nano scanner without and with the pre-filter

Finally, the performance of the proposed pre-filter is investigated by measuring the AFM image. The images are obtained for the conditions when the pre-filter is not used [Fig. 5(a)] and used [Fig. 5(b)] for lateral scanner with the vertical scanner controller gain adjusted to be stable. The scan range is 50x50 um and scan time is set to 180 s in each image. The magnitude of the vibration, 65 nm is observed in Fig. 5(a). On the contrary, the vibration magnitude is below 1 nm in Fig. 5(b). We can verify the z axis vibration which arises from the resonance effect of the nano scanner is almost disappeared.

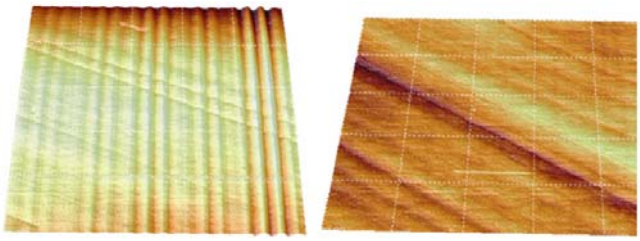

(a) The pre-filter is not used (b) The pro-filter is used

Fig. 5 Measured bare wafer images

5. Conclusions

In order to solve the vibration problem of the VCM nano scanner, the pre-filter is applied with the consideration of the disturbance and the electronic noise caused by the controlled signal to the VCM nano scanner. The vibration problem is disappeared in the experimental results as seen in the time domain and frequency domain, and a measured bare wafer image.

The VCM nano scanner can be expanded for use to the application for the wide working range and control without using the external sensor, and reasonable working speed range to a few hundred Hertz.

ACKNOWLEDGEMENTS

This work was supported by Research Center for Biomolecular Nanotechnology at GIST, in 2009 and the Korea Research Foundation Grant funded by the Korean Government (MOEHRD, Basic Research Promotion Fund) (KRF-2007-313-D00028).

REFERENCES

1. Wildeer, K., Quate, C. F., Singh, B. and Kyser, D. F., "Electron beam and scanning probe lithography: a comparision," J. Vac. Sci. Technol. B, Vol. 16, No. 6, pp. 3864-3873, 1998.
2. Betzig, E., Trautman, J. K., Wolfe, R., Gyorgy, E. M., Finn, P. L., Kryder, M. H. and Cahang, C. H., "Near-field magneto-optic and high density data storage," Appl. Phys. Lett., Vol. 61, No. 2, pp. 142-144, 1992.
3. Lee, D.-J., Lee, K.-K., Park, N.-C. and Park, Y.-P., "Development of 3-axis Nano scanner for precision positioning in lithography system," Processing of the IEEE, International Conference on Mechatronics &Automation, Vol. 3, pp. 1598-1603, 2005.
4. Kajihara, Y., Takeuchi, T., Takahashi, S. and Takamasu, K., "Development of an in-process confocal positioning system for nano-stereolithography using Evanescent Light," International Journal of Precision Engineering and Manufacturing, Vol. 9, No. 3, pp. 51-54, 2008.
5. Park, J. S. and Jeong, K. W., "A study of the design and conrol system for the ultra-precision stage," Proceedings of the KSMTE Spring Conference, pp. 54-59, 2005.
6. Mori, K., Munemoto, T., Otsuki, H., Yamaguchi, Y. and Akagi, K., "A dual-stage magnetic disk drive actuator using a piezoelectric device for a high track density," IEEE Trans. on Magnetics, Vol. 27, No. 6, pp. 5298-5300, 1991.
7. Kweon, H. K., "A New Calibration Method of Atomic Force Microscopy," International Journal of the Korean Society of Precision Engineering, Vol. 2, No. 2, pp. 11-16, 2001.
8. Jung, H. W. and Gweon, D.-G., "Creep characteristics of PZT stack actuator," Review of Scientific Instruments, Vol. 71. No. 4, pp. 1896-1900, 2000.
9. Kim, H.-S., Lee, B.-R. and Park, K.-Y., "Precision Position Control of a Piezoelectric Actuator Using Neural network," J. of KSPE, Vol. 16, No. 11, pp. 9-15, 1999.
10. Hong, S. R. and Lee, B. R., "Ultra-Precision Control of Piezoelectric Actuator System Using Hysteresis Compensation," Proceeding of the KSPE Autumn Conference, pp. 85-88, 2000.
11. Bloch, F., Lhermet, N., Meneround, P. and Claeyssen, F., "Space Compliant Moving Coil Actuator," 9th International Conference on New Actuators, pp. 661-664, 2004.
12. Encica, L., Makarovic, J., Lomonova, E. A. and Vandenput, A. J. A., "Space Mapping Opimawation of a Cylinderical Voice Coil Actuator," IEEE Trans. on Industry Applications, Vol. 42, No. 6, pp. 1437-1444, 2006.
13. Kwon, K. H., Oh, S. H., Cho, N. G. and Yoon, J. Y., "Development of small loading and Positioning Device using VCM," J. of KSPE, Vol. 20, No. 12, pp. 64-72, 2003.
14. Lee, S.-Q., Kim, E.-K., Youm, W.-S., Park, K.-H., Park, K.-H. and Chetwynd, D., "Bi-direction controllable AFM head driven by VCM with flexure hinge," Proc. of 4th euspen International Conference European Society for Precision Engineering and Nanotechnology, pp. 83-85, 2004.
15. Youm, W. S., Lee, S.-Q. and Park, K. H., "Optimal design and control of a voice coil motor driven flexure hinge for AFM actuator," Proc. of AIM, pp. 325-328, 2005.